Kidney International, Vol. 55 (1999), pp. 890–898

Proteinuria induces tubular cell turnover: A potential mechanism for tubular atrophy

Mark E. Thomas, Nigel J. Brunskill, Kevin P.G. Harris, Elaine Bailey, J. Howard Pringle, Peter N. Furness, and John Walls

Department of Nephrology, Department of Pathology, and Department of Cell Physiology and Pharmacology, Leicester General Hospital and University of Leicester School of Medicine, Leicester, England, United Kingdom

Proteinuria induces tubular cell turnover: A potential mechanism for tubular atrophy.

Background. Proteinuria and tubular atrophy have both been closely linked with progressive renal failure. We hypothesized that apoptosis may be induced by tubular cell exposure to heavy proteinuria, potentially leading to tubular atrophy. Apoptosis was studied in a rat model of "pure" proteinuria, which does not induce renal impairment, namely protein-overload proteinuria.

Methods. Adult female Lewis rats underwent intraperitoneal injection of 2 g of bovine serum albumin (BSA, $N = 16$) or sham saline injections (controls, $N = 8$) daily for seven days. Apoptosis was assessed at day 7 in tissue sections using *in situ* end labeling (ISEL) and electron microscopy. ISEL-positive nuclei (apoptotic particles) were counted in blinded fashion using image analysis with NIH Image. Cell proliferation was assessed by detection of mRNA for histone by *in situ* hybridization, followed by counting of positive cells using NIH Image.

Results. Animals injected with saline showed very low levels of apoptosis on image analysis. BSA-injected rats had heavy proteinuria and showed both cortical and medullary apoptosis on ISEL. This was predominantly seen in the tubules and, to a lesser extent, in the interstitial compartment. Overall, the animals injected with BSA showed a significant 30-fold increase in the number of cortical apoptotic particles. Electron microscopy of tubular cells in a BSA-injected animal showed a progression of ultrastructural changes consistent with tubular cell apoptosis. The BSA-injected animals also displayed a significant increase in proximal tubular cell proliferation. This increased proliferation was less marked than the degree of apoptosis.

Conclusion. Protein-overload proteinuria in rats induces tubular cell apoptosis. This effect is only partially balanced by proliferation and potentially provides a direct mechanism whereby heavy proteinuria can induce tubular atrophy and progressive renal failure.

Proteinuria has recently been recognized as a possible direct mediator of progressive renal injury rather than as a passive marker of glomerular injury [1, 2]. Proteinuria is a key predictor of declining glomerular filtration rate in patients with chronic renal disease [3]. Tubulointerstitial injury has also been shown to be an important predictor of progressive renal failure. There are many potential mechanisms by which proteinuria could directly lead to tubulointerstitial injury [1]. Proteinuria in rats may result in tubular injury, as evidenced by proximal tubule droplet formation [4–9], brush border loss [7], tubular luminal cast formation [7, 9–11], and vimentin expression [8]. Tubular cell injury, manifested by N-acetyl-β-glucosaminidase release, is known to occur in proteinuric human glomerular disease in proportion to the degree of proteinuria [12]. The concurrence of tubular atrophy and proteinuria in progressive renal failure suggests that proteinuria could disturb the normal balance of tubular cell proliferation and death.

In contrast to the uncontrolled nature of necrotic cell death, apoptosis is cell suicide or cell death in a controlled fashion. It ultimately leads to recognition and phagocytosis of the affected cell, typically by macrophages. Other cells, such as fibroblasts and epithelial cells, may also phagocytose neighboring apoptotic cells [13]. The apoptotic process is rapid and difficult to detect with standard sections taken at a fixed time point [14]. Low-grade apoptosis may be difficult to detect, even when it is cumulatively responsible for extensive cell loss [13]. It also occurs in patchy clusters [14]. Thus, assessment of apoptosis may require examination of several thousand cells. Apoptosis of native tubulointerstitial cells in chronic proteinuric glomerular disease has not been well studied. Tubular cell apoptosis has been described in other chronic renal conditions [15]. Furthermore, tubular epithelial cells *in vitro* undergo apoptosis, for example, in response to sublethal injury with cisplatin [16]. Apoptosis may be a common or unified response to cellular insults, which are at a level insufficient to cause cell necrosis, and thus may be provoked by a variety of such insults [13].

We hypothesized that tubular atrophy in proteinuric

Key words: apoptosis, tubulointerstitial injury, albuminuria, progressive renal failure, protein overload proteinuria.

Received for publication March 20, 1998
and in revised form September 28, 1998
Accepted for publication September 28, 1998

states could be mediated by increased cell death due to apoptosis. In order to examine this hypothesis, we have examined both apoptosis and proliferation in the proteinuric renal disease, protein-overload proteinuria. This is a renal disease model manifest by heavy proteinuria without renal impairment and an absence of any recognized classic immune response [8].

METHODS

Protein overload nephropathy was induced as previously described [17]. Adult female Lewis rats, weighing 174 ± 11 g (mean ± SD) at day 0, were used. Rats were allowed free access to water and standard rat chow. Rats were given seven daily intraperitoneal injections of 2 g of bovine serum albumin (BSA, $N = 17$, with 16 rats completing the protocol) or were injected with an equivalent volume of sterile normal saline as controls ($N = 8$). Blood samples were taken at baseline (day −7), days 2, 4, and 7 (at sacrifice), following the collection of a 24-hour urine specimen. At sacrifice, *in situ* perfusion of the kidneys with saline was carried out by aortic cannulation.

Bovine serum albumin (BSA) solution was prepared from Sigma preparation A4503, which has been used by others for this model [8]. BSA solution was prepared aseptically using 87 mmol/liter sodium hydroxide plus 65 mmol/liter sodium chloride solution in nanopure water as the diluent. Seventy-two grams of BSA powder were added per 100 ml of diluent. The mixture was shaken on an orbital shaker at 230 r.p.m., producing a BSA solution of approximately 40% (pH 6.5). Albumin concentration of the solution was assayed, the solution diluted to 33%, and aliquots stored at 4°C until the time of injection. Endotoxin levels in the BSA preparation were tested using a qualitative Limulus amoebocyte lysate assay kit (Endotect; ICN Biomedicals Ltd., Thame, Oxon, UK; maximum sensitivity 0.06 to 0.10 ng/ml of endotoxin). Neat BSA solution contained no detectable endotoxin.

Serum BSA was measured by radial immunodiffusion (The Binding Site Ltd., Birmingham, UK).

In situ end labeling (ISEL) for the detection of apoptosis was carried out on 4 μm formol saline-fixed, paraffin-embedded sections. The method used was that used by Gavrieli et al with minor modifications [14, 18]. In brief, sections were pretreated with 2 μg/ml proteinase K. Terminal deoxynucleotidyl transferase and digoxygenin-11-dUTP were added. Terminal deoxynucleotidyl transferase binds to the exposed 3′-OH ends of fragmented DNA and synthesizes a polydeoxynucleotide homopolymer (poly dU), incorporating digoxygenin-deoxyuridine. Sections were incubated with polyclonal sheep anti-digoxygenin/alkaline phosphatase conjugate, the signal visualized with nitroblue tetrazolium and 5-bromo-4-chloro-3-indolylphosphate, and counterstained with hematoxylin. Apoptotic cells, by virtue of having numerous free 3′-OH DNA ends, stained black, whereas normal cells took up only the lighter counterstain.

The program NIH Image (version 1.57) was used to analyze video images of the sections, using a Carl Zeiss III RS microscope with a JVC TK 1280E video camera, which was linked to an Apple MacIntosh Power PC. The techniques were adapted from our previously published work [19]. Sections were viewed at ×125 under constant lighting. Using a graticule, each ×125 field was shown to measure approximately 0.18 mm^2. Preliminary work suggested that the apoptotic process was quite patchy and difficult to count by eye at high power (data not shown). Therefore, NIH Image was used to perform blinded particle counts for ISEL-positive particles on coded sections. Ten cuts per section were counted, each with four adjacent, nonoverlapping fields, progressing perpendicularly from subcapsular (field 1) to inner cortex/outer medulla (field 4). Staining of a size between 5 and 25 pixels (that is, the size of an apoptotic nucleus) was counted as a single particle. Only dense staining was counted, using a fixed high threshold of 160 in NIH Image. A median of 40 (range 20 to 44) low-power fields was counted per rat.

For electron microscopy, kidney cortex was fixed in 2% glutaraldehyde in phosphate-buffered saline. Tissue samples were postfixed in aqueous osmium tetroxide and were dehydrated and embedded in epoxy resin. Ultrathin sections (70 to 90 nm) were cut on a Reichart-Jung OMU-4 ultramicrotome, contrasted with uranyl nitrate and lead citrate, and examined with a JEOL 100CX electron microscope.

Proliferating cells in the S phase of the cell cycle were detected by *in situ* hybridization for histone mRNAs using a technique already established in our laboratory [20]. A cocktail of digoxygenin-labeled oligonucleotide probes complementary to H2, H3, and H4 histone genes was applied to paraffin wax sections of kidneys derived from both control and experimental animals. After hybridization, sections were washed, and the *in situ* hybridization signal was detected using alkaline phosphatase-conjugated antidigoxygenin antibodies as previously described [20]. Brown/black staining of the cytoplasm indicated that the cell was in S phase. NIH Image was used to perform blinded particle counts for S Histone mRNA-positive cells on coded sections. Typically, 10 cuts per section were counted, each with four adjacent, nonoverlapping fields (as for analysis of ISEL mentioned earlier here). Staining of a size between 15 and 300 pixels (that is, the size of positive cell cytoplasm), above a fixed high threshold of 210, was counted as a single particle. A median of 40 (range 28 to 48) low-power fields (approximately 0.17 mm^2) was counted per rat.

Statistical analysis was carried out using Minitab Statistical software (Release 9; Minitab Inc., State College,

Table 1. Serum and urine chemistries

Serum values	Group	Day −7	Day 2	Day 4	Day 7
Creatinine *umol/liter*	BSA	45 ± 7	46 ± 7	40 ± 18	45 ± 24
	Saline	35 ± 5	27 ± 8	27 ± 2	15 ± 3
P		0.01	< 0.002	> 0.3	0.01
Total protein *g/liter*	BSA	63 ± 2	80 ± 6	77 ± 4	77 ± 3
	Saline	59 ± 2	56 ± 3	62 ± 3	58 ± 3
P		0.02	< 0.001	< 0.001	< 0.001
BSA by RID, *g/liter*	BSA	ND	61 ± 16	69 ± 17	52 ± 18
	Saline	ND	ND	ND	ND
Urine values	**Group**	**Day −8**	**Day 1**	**Day 3**	**Day 6**
Creatinine clearance *ml/min*	BSA	1.1 ± 0.3	1.0 ± 0.2	1.5 ± 0.8	1.6 ± 1.1
	Saline	1.5 ± 0.5	2.3 ± 1.0	2.2 ± 0.5	3.7 ± 1.2
P		0.30	0.07	0.19	0.01
Urinary protein *mg/24 hr*	BSA	3.4 ± 0.7	956 ± 476	1140 ± 229	849 ± 258
	Saline	6.7 ± 4.5	7.4 ± 3.2	5.8 ± 1.9	3.8 ± 2.0
P		0.04	< 0.001	< 0.001	< 0.001

Values are mean ± standard deviation. *P* values were calculated by the Mann-Whitney test adjusted with Bonferroni's correction. ND is not done.

PA, USA). Kruskal–Wallis analysis of variance and Mann–Whitney tests were used for nonparametric distributions. Cuzick's nonparametric test for trend across ordered groups was used as described [21]. Bonferroni's correction was used for multiple testing. Boxplots show the median line, interquartile range (marked by the box edges), and range of data (shown by the whiskers).

RESULTS

Serum and urine biochemistry

Serum and urine biochemical parameters are shown in Table 1. The BSA injections produced a marked and prompt rise in serum total protein and serum BSA levels. Thus, in the BSA group, serum total protein levels rose by a median of 28% between baseline and day 2, and albumin rose by a median of 44% (with an assay that measured both rat albumin and BSA). The BSA group had no significant change in creatinine levels (baseline vs. day 7, $P > 0.6$), whereas the saline group had a significant fall in creatinine (mean fall 57%, baseline vs. day 7, $P < 0.002$, Mann–Whitney). The fall may have been due to the volume-loading effect of the saline injection (approximately 7 ml/day). In the BSA-injected animals, creatinine clearance (C_{Cr}) rose by approximately 30%, but was not significantly different between baseline and day 7 ($P > 0.7$, Mann–Whitney). In the saline-injected animals, the C_{Cr} rose by approximately 150% during the experimental period (Table 1) and was significantly increased at day 7 compared with baseline ($P < 0.003$). The BSA-injected group had gross proteinuria approaching 1000 mg/day, or half of the daily injected dose (Table 1). These results are comparable to previous studies of this model [17].

Apoptosis measured by *in situ* end labeling

Figure 1 shows photomicrographs of ISEL of renal cortex from rats injected with BSA (Fig. 1A) or saline (Fig. 1B). Apoptosis is seen in animals injected with BSA but not in those injected with saline. In Figure 1A, this is seen as a number of tubular nuclei that show intense black ISEL staining, in contrast to the surrounding normal tubular nuclei with visible nucleoli. Even on this section, with active apoptosis, it can be seen to be a patchy process. Apoptosis was also seen in the medulla of rats injected with BSA but not in those injected with saline (not shown).

Quantitation of ISEL stained apoptotic particles, in blinded fashion, demonstrated that the animals injected with saline showed very low levels of apoptosis. Rats injected with BSA showed significantly more apoptotic particles compared with animals injected with saline (Fig. 2A). In BSA-injected rats, there appeared to be increasing numbers of apoptotic particles from the outermost cortex (field 1) to the inner cortex/outer medulla (field 4; Fig. 2B). However, there was no evidence of a significant trend across the four fields using Cuzick's test ($P = 0.8$). There was a constant, very low level of apoptosis across the cortex in saline-injected animals (Fig. 2B). Apoptosis within the BSA-injected group did not show any correlation with proteinuria levels on day 3 or day 6.

Electron microscopy

Transmission electron microscopy was used as a qualitative method to look for evidence of apoptosis in the BSA-injected group. It was also used to study the ultrastructural changes of apoptosis in tubular epithelial cells *in vivo*, as these have not been previously described with proteinuria. Normal tubular cells showed nuclei with the usual open or dispersed pattern of nuclear chromatin (Fig. 3A). At an early stage of apoptosis, tubular cells in the BSA group showed peripheral clumping or condensation of chromatin along the inner face of the nuclear membrane (Fig. 3 B, D, left hand tubular cell). In

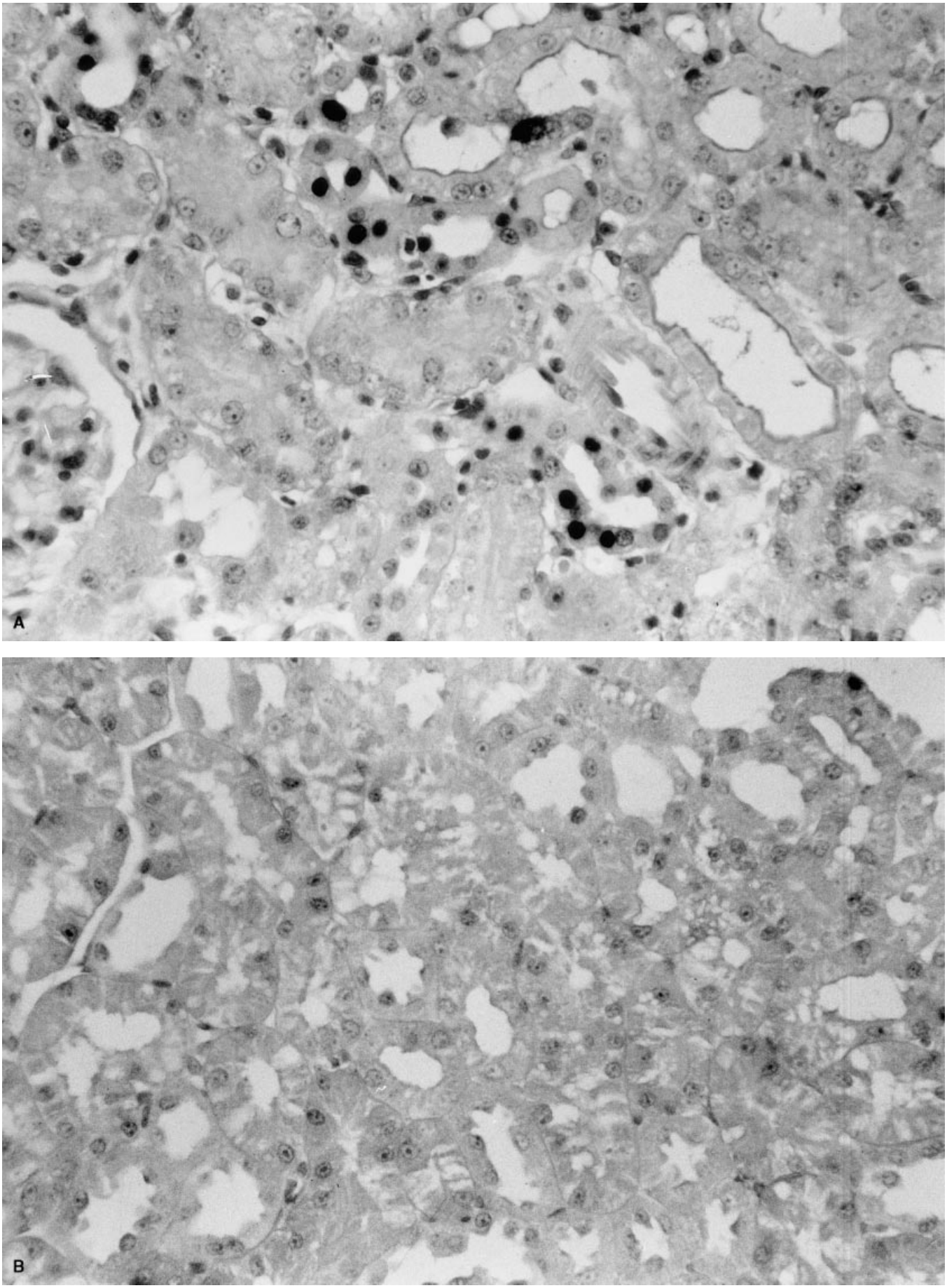

Fig. 1. *In situ* end labeling of apoptotic cells. (*A*) Animal injected with BSA: cortex, ×526. (*B*) Animal injected with saline: cortex, ×526.

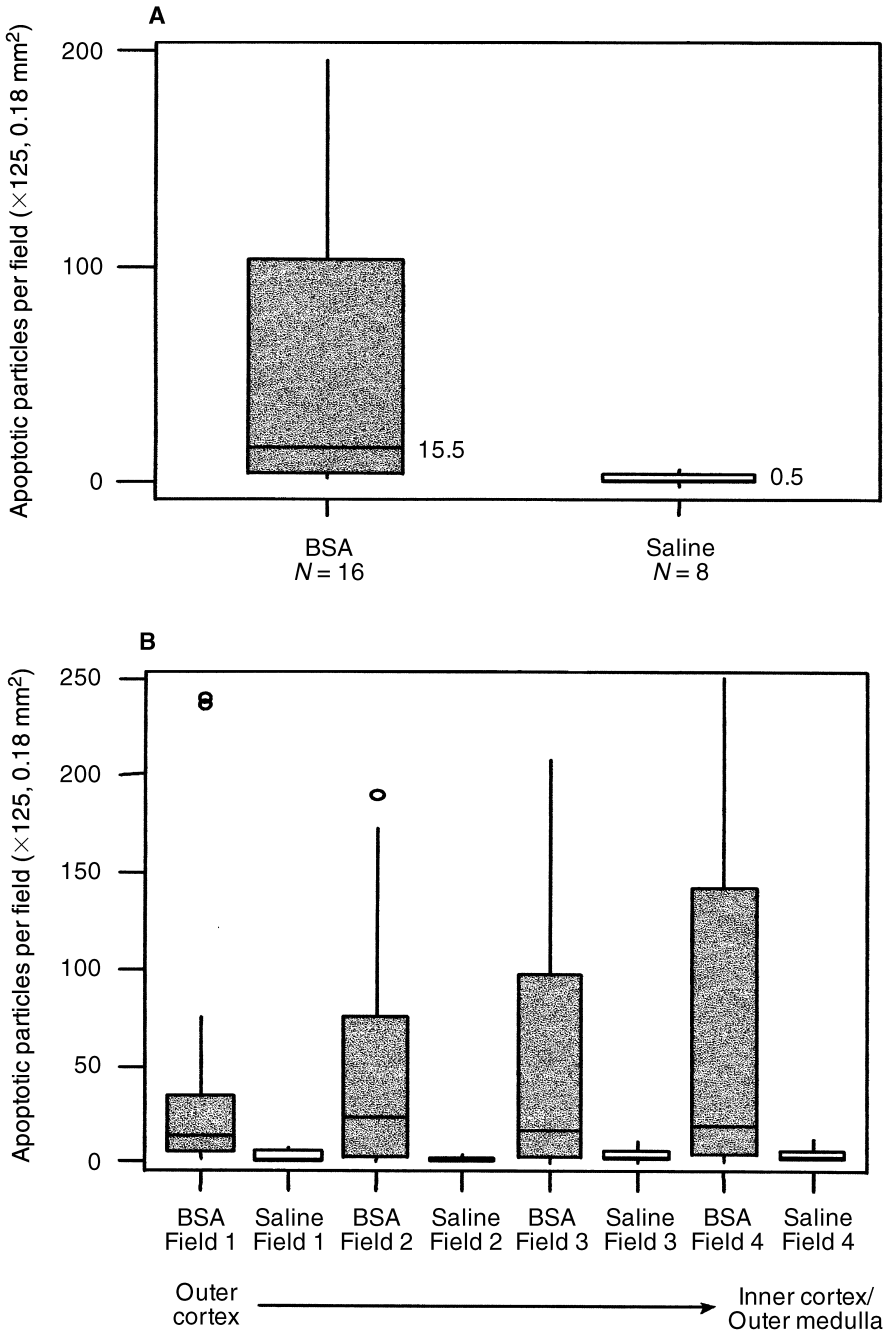

Fig. 2. Apoptosis quantified by *in situ* end labeling. Boxplots show the median line, interquartile range (box) and range. Numbers in panel A are the median values. (*A*) All fields, $P = 0.002$, BSA versus saline (Mann-Whitney test). (*B*) Apoptosis at different levels in the cortex and outer medulla, $P < 0.01$, BSA versus saline for each field (Man-Whitney test with Bonferroni's correction. Symbol (◦) indicates an outlier.

addition, early nuclear shrinkage was present at this stage. At a later stage (Fig. 3C), the peripheral chromatin condensation and nuclear shrinkage were more marked. Some of the perinuclear electron dense structures may represent apoptotic bodies. The most advanced stage of apoptosis seen in these studies is shown in the tubular cell on the right hand side of Figure 3D. The condensed chromatin shows a vacuolated appearance. The nature of these vacuoles is uncertain, but they may represent detached nuclear pores, or alternatively, they may be splicosomes. In spite of the nuclear condensation, the cytoplasmic structures remained intact.

Cell proliferation determined by histone mRNA *in situ* hybridization

Cell proliferation was measured using the same particle counting technique in NIH Image employed for ISEL, with fields of comparable size. Examination of kidney sections derived from control animals revealed detectable but very low levels of proliferating cells in

the cortex. Proteinuric animals, however, demonstrated a significant increase in S-phase cells in the cortex (Table 2). The magnitude of increase in proliferation was not as great as the increase in apoptosis demonstrated in the same animals.

DISCUSSION

To date, there have been no studies of apoptosis in rat models of proteinuric renal disease. This is the first description of apoptosis in such a model, namely heterologous protein-overload proteinuria. The BSA preparations were prepared under aseptic conditions and were shown to have undetectable endotoxin levels. This model specifically causes modest nonimmune glomerular injury and pure heavy proteinuria without renal impairment. The proteinuria occurs because of a combination of the glomerular injury plus the accompanying albumin overload. No evidence of any classic humoral or cell-mediated immune response has ever been demonstrated in this model. In particular, antibodies to heterologous albumin are not seen.

The protein-injected group had massive proteinuria, which was of similar magnitude to that previously reported [17]. Saline-injected animals showed a clear rise in C_{Cr}, probably because of the volume-loading effect of saline. The inclusion of albumin in the injection reduced this rise in C_{Cr}. This suggests that some degree of renal injury exists in the BSA-injected animals, counteracting the rise in glomerular filtration rate induced by saline loading.

Apoptosis was measured by ISEL. In order to make this technique more specific for apoptosis, the method of Gavrieli et al was modified by reducing the concentration of proteinase K used in pretreatment of tissue sections [14]. As such, ISEL is much less likely to label necrotic or other nonapoptotic cells. Furthermore, by counting only the most intensely stained cells with NIH Image, confusion with nonapoptotic cells is lessened.

There was a very low background level of apoptosis in the control animals, in the large fields examined by ISEL and image analysis. This is in agreement with previous studies of normal rat kidneys [22]. Animals injected with BSA showed significantly more apoptotic particles compared with animals injected with saline. Apoptosis was apparent in both the cortex and medulla of BSA-injected animals. Although we did not quantitate apoptosis across the entire medulla, the clear occurrence of apoptosis across the cortex, including the inner cortex/outer medulla (Fig. 2B), also suggests that there is notable apoptosis in the medulla.

Apoptosis, when measured in standard tissue sections at a given time point, is a subtle process that is difficult to detect [13]. Although this study found a median of only 15 apoptotic particles per low-power (0.18 mm^2) field in the BSA-injected group, this was 30-fold higher than the number found in the saline-injected group (a median of 0.5 per field). Moreover, owing to the rapidity of apoptosis, even at an apparently low level, it can represent substantial cellular loss [13]. Such an increase in apoptosis could disturb the normal balance between tubular cell proliferation and death, leading to tubular atrophy, a key feature of progressive proteinuric renal disease.

The morphological features of tubular cell apoptosis *in vivo* have not been well described. Polarized epithelial cells may have distinctive, somewhat "atypical," morphological features when they undergo apoptosis. In rat distal tubular epithelial cells exposed to a thiazide diuretic, apoptosis is accompanied by a loss of tight junctions, wide intercellular spaces, heavy chromatin condensation, and "apoptotic bodies" [23]. We have similarly found evidence of chromatin condensation and possible apoptotic bodies in this study, and the electron microscopic appearances of tubular apoptosis we describe are similar to those presented in the work of Loffing et al [23].

A number of apoptotic cells are observed in the interstitium of the kidney in addition to those observed in the tubules themselves. The precise identity of these cells is uncertain. One possibility is that apoptotic tubular cells may be engulfed by phagocytic macrophages resident in the interstitium. Alternatively, interstitial macrophages themselves may be subject to apoptosis, as, of course, may other unidentified interstitial cells. Currently, the fate of the apoptotic tubular cells remains to be determined.

Preservation of tissue mass depends on the maintenance of a balance between the rate of cell death and the rate cell proliferation. Our study has demonstrated a significant proliferative response in the proximal tubule of proteinuric animals. However, the degree of proliferation observed is considerably less than the degree of apoptosis occurring in the same areas of the kidney. The significance of this observation is that apoptosis is apparently not balanced by proliferation, and hence, the net result is likely to be deletion of cells. This deleterious situation may explain, at least in part, the tubular atrophy observed in proteinuric states.

Apoptosis in a variety of kidney conditions may be a prototypical response to nonlethal cellular insults. Thus, proteinuria may not be a unique stimulus to apoptosis in the kidney [15, 24, 25]. However, proteinuria is probably the most important stimulus to apoptosis in chronic renal disease. It is hypothesized, based on these results, that proteinuria provokes a shift in favor of apoptosis, which ultimately may lead to tubular atrophy. The lack of correlation of apoptosis with proteinuria might be viewed as evidence against this hypothesis. However, measured levels of excreted urine proteins do not reflect the much higher levels to which the tubules are exposed [26]. Furthermore, this study was not designed to test

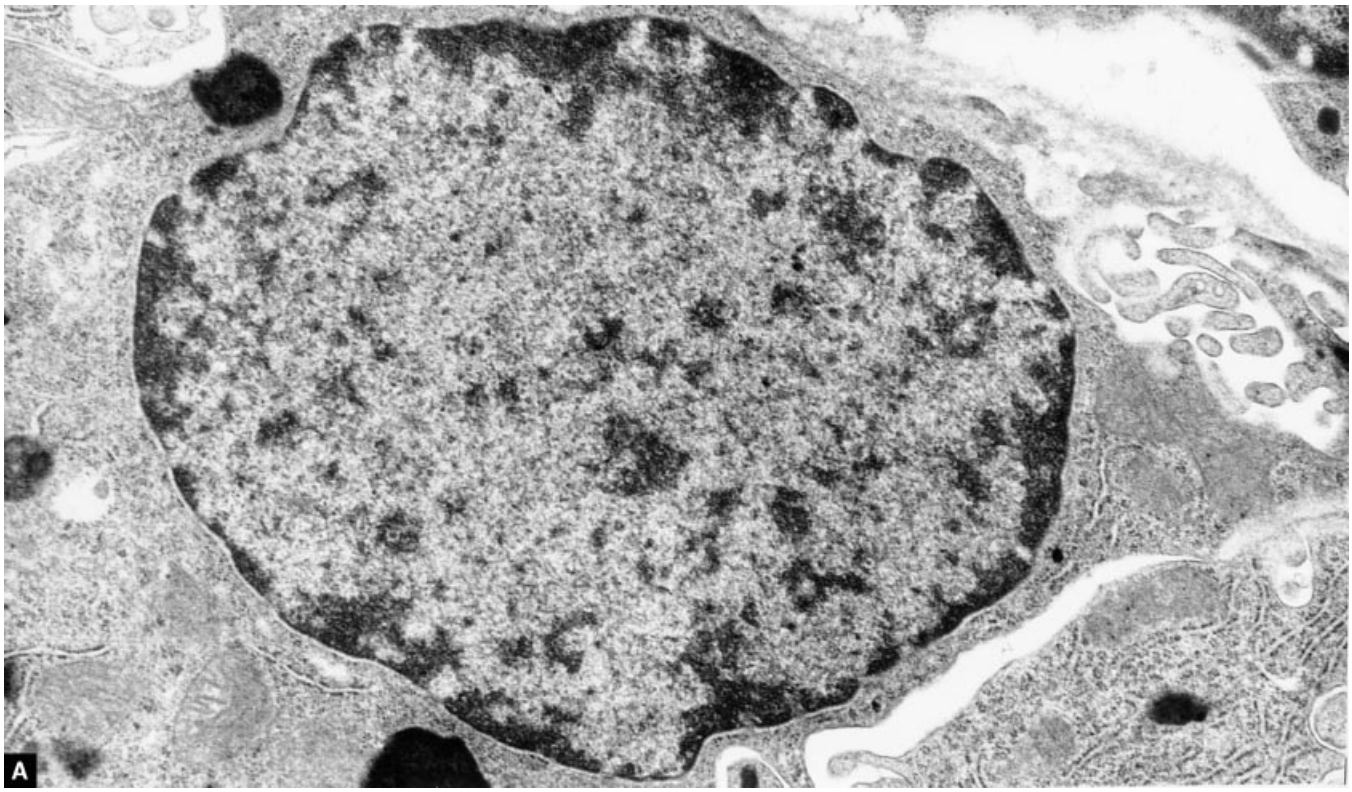
A

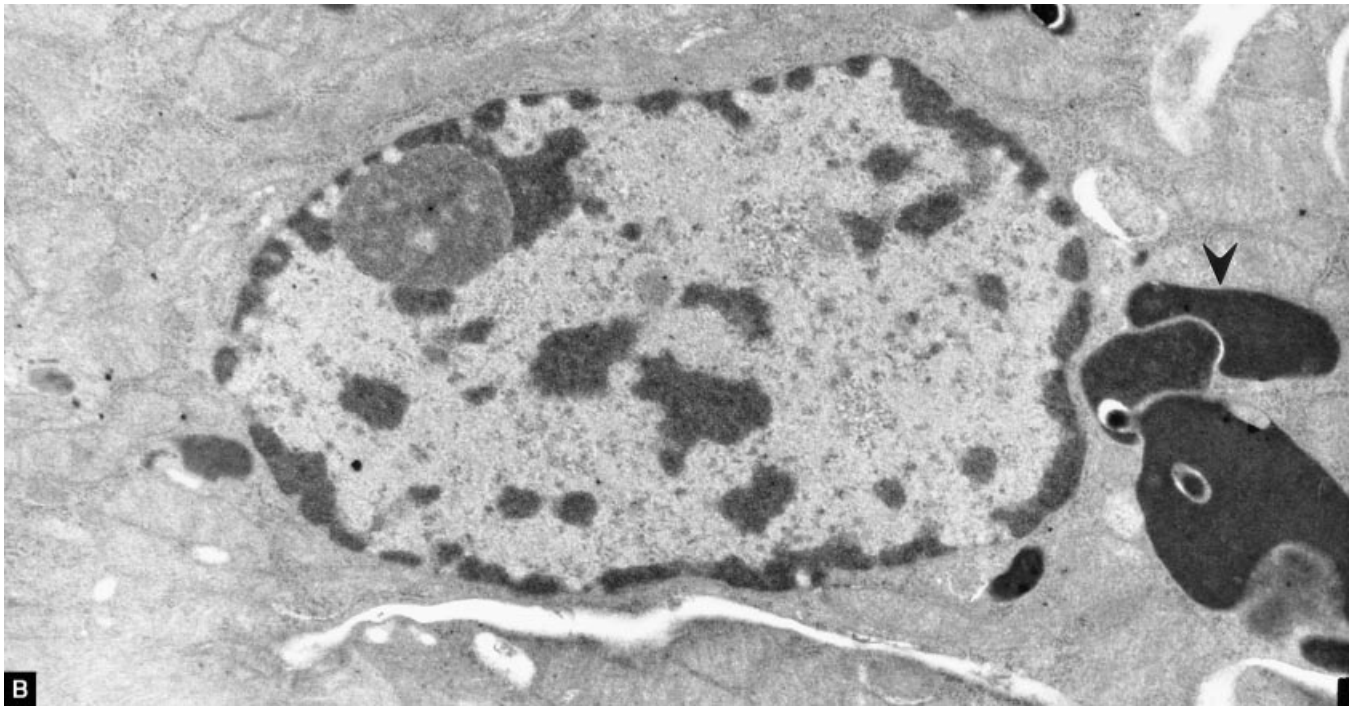
B

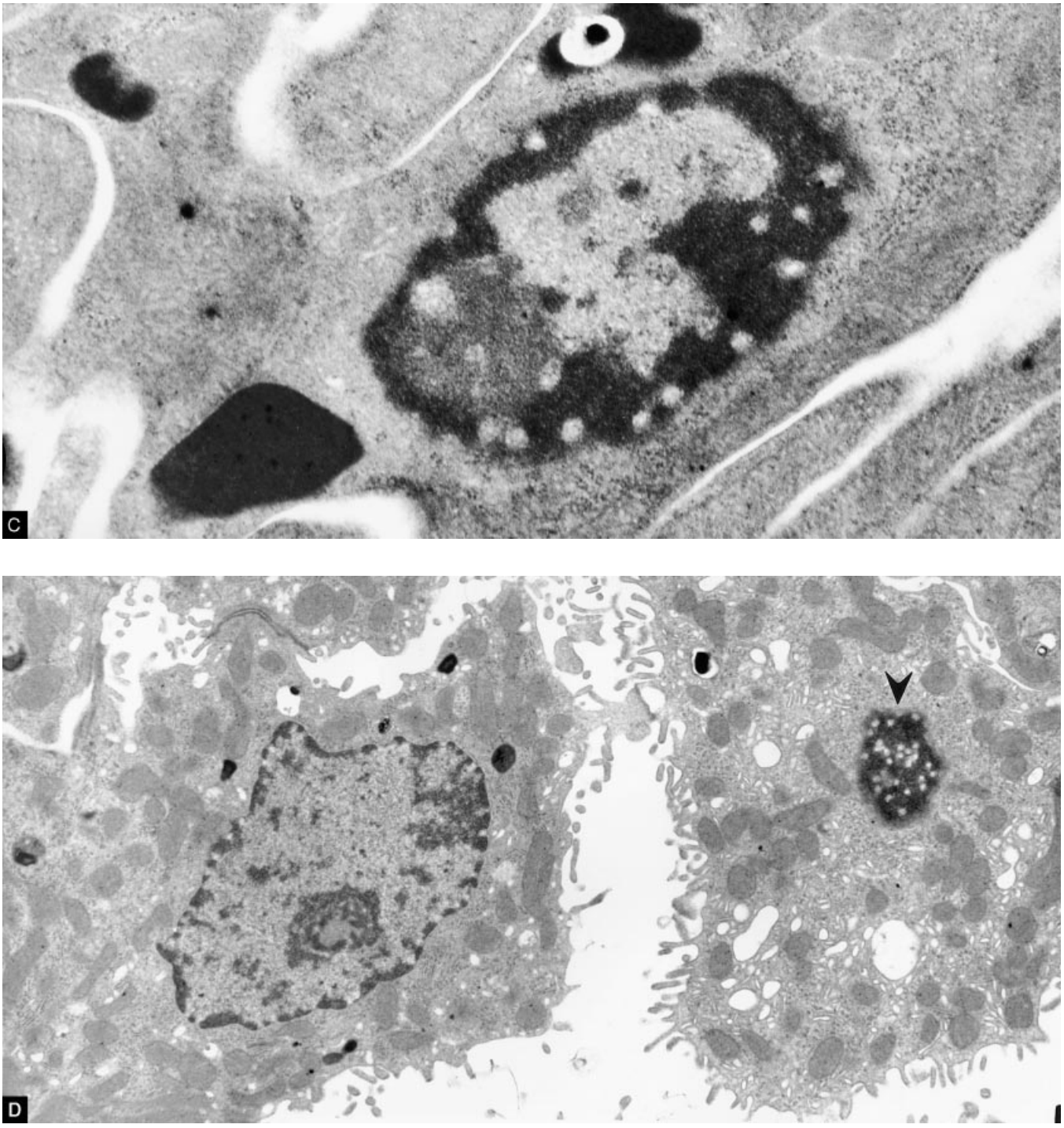

Fig. 3. Transmission electron microscopy of apoptotic tubular cells in an animal injected with BSA. (*A*) Tubular cells showing normal morphology with dispersed nuclear chromatin (×28,727). (*B*) Tubular cell showing early peripheral clumping of nuclear chromatin and possible apoptotic bodies (arrow; ×23,196). (*C*) Tubular cell showing a later stage of apoptosis with nuclear shrinking and chromatin condensation (×45,431). (*D*) Two tubular cells showing possible early apoptosis and neighbor cell with late stage apoptosis (arrow to condensed nucleus; ×14,009).

Table 2. Cortical S histone mRNA *in situ* hybridization

Group	BSA injected rats ($N = 8$)	Saline injected rats ($N = 9$)	P
S histone mRNA positive cells per 0.17 mm^2 field	9.3 ± 9.6	0.3 ± 0.5	0.009

Values are mean ± standard deviation. P value is shown (Mann-Whitney test).

the effect of different doses of injected BSA on the level of renal apoptosis.

In conclusion, this work has provided new evidence that albuminuria increases tubular cell turnover manifest as both apoptosis and proliferation. The balance, however, favors the development of tubular atrophy, one of the histologic hallmarks of chronic renal failure. This study provides evidence of a direct *in vivo* link between proteinuria and tubulointerstitial injury, two key factors [27, 28] in the progression of renal disease.

ACKNOWLEDGMENTS

Dr. Brunskill is supported by a Wellcome Trust Advanced Fellowship. This work was presented at the American Society of Nephrology meeting at San Antonio, Texas, in November 1997. Dr. Steve Harper kindly assisted with the *in situ* hybridization. We are grateful to Jes Brown and Frease Baker for technical assistance, and Dr. G. Willars, Department of Cell Physiology and Pharmacology, University of Leicester, for statistical advice. NIH Image was kindly supplied by Wayne Rasband, National Institutes of Health.

Reprint requests to Dr. Mark Thomas, Department of Renal Medicine, Birmingham Heartlands Hospital, Bordesley Green East, Birmingham, B9 5SS, England, United Kingdom.

REFERENCES

1. Remuzzi G, Ruggenenti P, Benigni A: Understanding the nature of renal disease progression. *Kidney Int* 51:2–15, 1997
2. Thomas ME, Schreiner GF: The contribution of proteinuria to progressive renal injury: The consequences of tubular uptake of fatty acid bearing albumin. *Am J Nephrol* 13:385–398, 1993
3. Peterson JC, Adler S, Burkart JM, Greene T, Hebert LA, Hunsicker LG, King AJ, Klahr S, Massry SG, Seifter JL, Modification of Diet in Renal Disease (MDRD) Study Group: Blood pressure control, proteinuria, and the progression of renal disease: The Modification of Diet in Renal Disease Study. *Ann Intern Med* 123:754–762, 1995
4. Lannigan R, McQueen EG: The effect on the renal glomerular epithelial cells of proteinuria induced by infusions of human serum albumin in rabbits and rats. *Br J Exp Pathol* 43:549–555, 1958
5. Ashworth CT, James JA: Glomerular excretion of macromolecular substances. *Am J Pathol* 39:307–316, 1961
6. Anderson MS, Recant L: Fine structural alterations in the rat kidney following intraperitoneal bovine albumin. *Am J Pathol* 40:555–569, 1962
7. Andrews PM: A scanning and transmission electron microscopic comparison of puromycin aminonucleoside-induced nephrosis to hyperalbuminemia-induced proteinuria with emphasis on kidney podocyte pedicel loss. *Lab Invest* 36:183–197, 1977
8. Eddy AA, McCulloch L, Adams J, Liu E: Interstitial nephritis induced by protein-overload proteinuria. *Am J Pathol* 135:719–733, 1989
9. Bertani T, Cutillo F, Zoja C, Broggini M, Remuzzi G: Tubulointerstitial lesions mediate renal damage in adriamycin glomerulopathy. *Kidney Int* 30:488–496, 1986
10. Marks MI, Drummond KN: Nephropathy and persistent proteinuria after albumin administration in the rat. *Lab Invest* 23:416–420, 1970
11. Davies DJ, Brewer DB, Hardwicke J: Urinary proteins and glomerular morphometry in protein overload proteinuria. *Lab Invest* 38:232–243, 1978
12. Kunin CM, Chesney RW, Craig WA, England AC, Deangelis C: Enzymuria as a marker of renal injury and disease: Studies of N-acetyl-β-glucosaminidase in the general population and in patients with renal disease. *Pediatrics* 62:751–760, 1978
13. Lieberthal W, Levine JS: Mechanisms of apoptosis and its potential role in renal tubular epithelial cell injury. *Am J Physiol* 271:F477–F488, 1996
14. Gavrieli Y, Sherman Y, Ben-Sasson SA: Identification of programmed cell death in situ via specific labelling of nuclear DNA fragmentation. *J Cell Biol* 119:493–501, 1992
15. Truong LD, Petrusevska G, Yang G, Gurpinar T, Shappell S, Lechago J, Rouse D, Suki WN: Cell apoptosis and proliferation in experimental chronic obstructive uropathy. *Kidney Int* 50:200–207, 1996
16. Lieberthal W, Triaca V, Levine J: Mechanisms of death induced by cisplatin in proximal tubular epithelial cells: Apoptosis vs. necrosis. *Am J Physiol* 270:F700–F708, 1996
17. Kees-Folts D, Sadow JL, Schreiner GF: Tubular catabolism of albumin is associated with the release of an inflammatory lipid. *Kidney Int* 45:1697–1709, 1994
18. Kiberu SW, Pringle JH, Sobolewski S, Murphy P, Lauder I: Correlation between apoptosis, proliferation and bcl-2 expression in malignant non-Hodgkin's lymphoma. *J Clin Pathol Mol Pathol* 49:M268–M272, 1996
19. Furness PN, Rogers-Wheatley L, Harris KP: Semiautomatic quantitation of macrophages in human renal biopsy specimens in proteinuric states. *J Clin Pathol* 50:118–122, 1997
20. Jones PH, Harper SJ, Watts F: Stem cell patterning and fate in human epidermis. *Cell* 80:83–93, 1995
21. Altman DG: Comparing groups: Continuous data, in *Practical Statistics for Medical Research*, London, Chapman and Hall, 1991, p 177
22. Polzar B, Zanotti S, Stephan H, Rauch F, Peitsch MC, Irmler M, Tschopp J, Mannherz HG: Distribution of deoxyribonuclease I in rat tissues and its correlation to cellular turnover and apoptosis (programmed cell death). *Eur J Cell Biol* 64:200–210, 1994
23. Loffing J, Loffing-Cueni D, Hegyi I, Kaplan MR, Hebert SC, Le Hir M, Kaissling B: Thiazide treatment of rats provokes apoptosis in distal tubule cells. *Kidney Int* 50:1180–1190, 1996
24. Bodi I, Abraham AA, Kimmel PL: Apoptosis in human immunodeficiency virus-associated nephropathy. *Am J Kidney Dis* 26:286–291, 1995
25. Laine J, Etelamaki P, Holmberg C, Dunkel L: Apoptotic cell death in human chronic renal allograft rejection. *Transplantation* 63:101–105, 1997
26. Bernard DB: Nephrology forum: Extrarenal complications of nephrotic syndrome. *Kidney Int* 33:1184–1202, 1988
27. Risdon RA, Solper JC, De Wardener HE: Relationship between renal function and histological changes found in renal biopsy specimens from patients with persistent glomerular nephritis. *Lancet* 2:363–366, 1968
28. Schainuck LI, Striker GE, Cutler RE, Benditt EP: Structural-functional correlations in renal disease. Part II. The correlations. *Hum Pathol* 1:631–640, 1970